New Phytologist

Research

Resilience to seasonal heat wave episodes in a Mediterranean pine forest

Fedor Tatarinov[1], Eyal Rotenberg[1], Kadmiel Maseyk[1], Jérôme Ogée[2], Tamir Klein[1] and Dan Yakir[1]

[1]Earth & Planetary Sciences, Weizmann Institute of Science, Rehovot 76100, Israel; [2]UMR 1391 ISPA, INRA, Villenave dOrnon 33140, France

Author for correspondence:
Dan Yakir
Tel: +972 89342549
Email: dan.yakir@weizmann.ac.il

Received: *5 September 2015*
Accepted: *2 November 2015*

New Phytologist (2015)
doi: 10.1111/nph.13791

Key words: Aleppo pine (*Pinus halepensis*), drought, ecosystem activities, ecosystem response, extreme environment, heat wave, resilience.

Summary

- Short-term, intense heat waves (hamsins) are common in the eastern Mediterranean region and provide an opportunity to study the resilience of forests to such events that are predicted to increase in frequency and intensity.
- The response of a 50-yr-old Aleppo pine (*Pinus halepensis*) forest to hamsin events lasting 1–7 d was studied using 10 yr of eddy covariance and sap flow measurements.
- The highest frequency of heat waves was *c*. four per month, coinciding with the peak productivity period (March–April). During these events, net ecosystem carbon exchange (NEE) and canopy conductance (g_c) decreased by *c*. 60%, but evapotranspiration (ET) showed little change. Fast recovery was also observed with fluxes reaching pre-stress values within a day following the event. NEE and g_c showed a strong response to vapor pressure deficit that weakened as soil moisture decreased, while sap flow was primarily responding to changes in soil moisture. On an annual scale, heat waves reduced NEE and gross primary productivity by *c*. 15% and 4%, respectively.
- Forest resilience to short-term extreme events such as heat waves is probably a key to its survival and must be accounted for to better predict the increasing impact on productivity and survival of such events in future climates.

Introduction

The current projections for global climate change forecast an increase in the intensity and frequency of extreme climatic events, such as droughts and heat waves (Reichstein *et al.*, 2013; Reyer *et al.*, 2013). In the temperate and boreal regions, the forest trees are typically adapted to a sufficient supply of water and moderate temperatures. Severe heat waves, such as those that occurred in 2003 and 2010, can lead in this case to a considerable decrease in gross primary productivity (GPP) and in net ecosystem CO_2 exchange (NEE), temporarily converting forest ecosystems from sinks to sources of CO_2 (Ciais *et al.*, 2005; Girard *et al.*, 2012) while increasing tree mortality (Allen *et al.*, 2010; Maslov, 2010; Tuzov, 2013) and wildfire frequency (Goldammer, 2010; Shvidenko & Schepaschenko, 2013). Such events induce a range of ecophysiological responses, but with different effects among tree species. For example, the annual stem basal area increment (BAI) of *Fagus sylvatica* decreased from 2.8% to 1.3%, whereas the BAIs of *Crapinus betulus* and *Acer campestre* were unaffected by heat waves (Leuzinger *et al.*, 2005). Severe drought may lead to the mass mortality of trees from the direct effects of the drought or indirectly from pest attacks (Maslov, 2010; Tuzov, 2013).

Less is known about the response of different forests and other ecosystems in warmer biomes in which heat waves occur regularly. In the semiarid regions where plants are regularly exposed to water and heat stress for extended parts of the year, increasing the intensity, frequency, or length of droughts can be critical for the survival of forests and other ecosystems (Bonan, 2008). In some studies, resistance to heat waves is observed (Klein *et al.*, 2014). To maintain a functional hydraulic system under dry conditions, some tree species may also respond with transient stomatal closures, but long-term adjustments, such as leaf shedding, changes in the xylem, and cell wall suberization, are also observed (Maseda & Fernandez, 2006; Breda & Badeau, 2008). This study was conducted in a stand of *Pinus halepensis* (Aleppo pine), which is a common tree species across the Mediterranean region (Neeman & Trabaud, 2000). This pine species survives in a wide range of environmental conditions, from sea level to 2600 m in elevation and from 200 to 1500 mm of annual precipitation. In semiarid climates, the trees are exposed to seasonal heat waves, particularly in spring during the short, peak productivity season, which might affect their overall productivity and survival (Klein *et al.*, 2013).

Heat waves in the Mediterranean region are often associated with winds that bring warm, dry air from the desert regions. In the Middle East, such weather events are termed 'hamsin' or 'sharav'. In other parts of the Mediterranean, similar phenomena are also called sirocco (Italy), samum (Morocco), and leveche (Spain). These events are more frequent in the transition seasons, particularly in the spring (Goldreich, 2003). The word 'hamsin'

originates from the Arabic word for 'fifty' according to the popular belief that hamsin events occur on *c.* 50 d yr^{-1}. The typical hamsin events are characterized by a sharp increase in the temperature and the vapor pressure deficit (VPD) to high values of *c.* 35°C and *c.* 6000 Pa, respectively, over a few days for events that typically last for 1–7 d. The events are followed by a rapid return to pre-event values (below 20°C and 1000 Pa) within a day or so, but in some cases, a rain event occurs in the first days following a hamsin event. Thus, there is no commonly accepted definition of a hamsin event (Goldreich, 2003). It can be defined by threshold temperature and humidity values (Gat, 1990) or by deviation from long-term mean values based on some threshold (Winstanley, 1972; Goldreich, 2003). Under hamsin conditions, air humidity decreases very rapidly, but such changes are in most cases too rapid for soil moisture to change significantly, which offers an opportunity to distinguish atmospheric from soil moisture deficit effects on plant activities.

An important aspect of hamsin events is their high frequency, specifically during the short active season in the semiarid environments (usually in spring; Maseyk *et al.*, 2008a). Would the stress effects associated with the heat waves be long-lasting, a few of these events could eliminate a large fraction of the productive season, enhancing tree mortality. Similarly, productivity and survival can be greatly impacted by the predicted increase in the frequency and intensity of extreme weather events (Reichstein *et al.*, 2013; Reyer *et al.*, 2013).

Here we quantify the resilience (i.e. the decline and recovery of key functions) to seasonal heat waves of a semiarid pine stand, and test the hypothesis that such resilience is a key factor in its annual scale productivity, with potential implications for its survival if the frequency of such events were to markedly increase.

Materials and Methods

Study site

The Yatir forest is located at the northern edge of the Negev desert (30°20′N, 35°03′E; 650 m above sea level; Rotenberg & Yakir, 2010), covers an area of *c.* 2800 ha and is dominated by Aleppo pine (*Pinus halepensis* Miller). The primary part of the forest was planted in the mid-1960s. The stand density is *c.* 300 trees ha^{-1}. The soil is a predominantly light brown Rendzina, 25–100 cm deep. Pine roots are concentrated mainly in upper 60 cm with the maximum fine root density in the 20–40 cm layer (Grünzweig *et al.*, 2007; Klein *et al.*, 2013). The climate is Mediterranean with prolonged summer drought periods from May to October (average daily temperature in July is 25°C) and with a winter period with moderate precipitation (mean annual 290 mm) and temperatures (*c.* 10°C in January (Grünzweig *et al.*, 2007); mean values for 1964–2006).

Measurement system

Begun in 2000, the eddy covariance (EC) and supplementary meteorological measurements were conducted continuously in the Yatir forest (Grünzweig *et al.*, 2007; Rotenberg & Yakir, 2010). The measurements were performed according to the Euroflux methodology (Aubinet *et al.*, 2000) and were part of the European EC sites quality assessment project (Göckede *et al.*, 2008). The concentrations of CO_2 and water vapor and the fluxes of NEE (conventionally indicated as negative fluxes, out of the atmosphere) and evapotranspiration (ET, conventionally indicated as positive fluxes into the atmosphere) were measured continuously using a combination of a sonic anemometer (Gill R-50; Gill Instruments, Lymington, UK) and a closed-path CO_2/H_2O infrared gas analyzer (IRGA, LI-7000; Li-Cor, Lincoln, NE, USA) with the inlet placed 18.7 m above ground. The sonic and IRGA variables were used to calculate the ecosystem water VPD as the difference between the air saturation humidity derived from the sonic air temperature (corrected for humidity effects by the EC software) and the ambient humidity measured directly by the IRGA.

Collected since 2005 (and on-going), soil moisture measurements are available for the depths of 5, 15, 30, 50, 70 and 125 cm (Raz Yaseef *et al.*, 2010). The measurements were conducted using time-domain reflectometry (TDR) sensors (Trime-PICO 64; IMKO, Ettlingen, Germany) in three pits at depths of 30, 70 and 125 cm. Additional soil moisture data in the upper 30 cm were collected using another TDR sensor (Campbell Scientific, Logan, UT, USA). All soil moisture data were integrated over a 30 min time step and synchronized with the eddy flux measurements.

Collected since 2004 (and ongoing), tree sap flow was also measured in eight to 24 trees in different years. During 2004–2006, a homemade heat-pulse system (Schiller, 2011; Ungar *et al.*, 2013) was used. Granier-type sensors have been used since 2005 (Granier, 1985), and additionally, after 2009, Cermak-type (Cermak *et al.*, 2004) sensors were used (Klein *et al.*, 2012). Sap flow upscaling from tree to stand level is described in Klein *et al.* (2016) and was performed by averaging sap flux density per unit stem cross-section area among sample trees for each 30 min interval and multiplying it by total stand basal area.

Upscaled sap flow (Q, in mm h^{-1}) was used in all further analyses to represent the daily tree transpiration T_r. Therefore, the calculations that required the use of T_r, including the canopy daytime conductance, g_c, and the apparent and intrinsic water-use efficiency (W and W_i, respectively) were performed only on a daily basis using daily GPP and Q values and daytime VPD mean values.

The canopy conductance to CO_2 (g_c) was calculated as follows (see e.g. Beer *et al.*, 2009):

$$g_c = Q \cdot P/(1.6 \cdot \mathrm{VPD}) \qquad \text{Eqn 1}$$

where Q and VPD are as noted earlier, P is the daily average atmospheric pressure, and 1.6 is the ratio of conductance to CO_2 and water (reflecting the higher molecular diffusivity of water). The observed g_c was corrected for the difference in the VPD between that measured above the canopy and that at the level of the leaf by the constant correction factor of 1.18, which was found suitable for our system as described in Klein *et al.* (2016). W (in g C kg^{-1} H_2O) was calculated as GPP/Q. W_i was defined as $W_i = \mathrm{GPP}/g_c$ (Farquhar *et al.*, 1989; Keenan *et al.*, 2013) and was calculated as:

$$W_i = W \cdot \mathrm{VPD} \qquad \text{Eqn 2}$$

Supplementary meteorological variables

Air temperature and humidity at 5 m above the canopy (15 m above ground) were measured with HMP45C sensor probes and an air pressure sensor (Campbell Scientific). Radiation measurements included atmospheric and ecosystem facing solar radiation (CM21; Kipp&Zonen, Delft, the Netherlands). All meteorological sensors were connected using a differential mode, and the data were stored as half-hourly means via multiplexers to data loggers (AM16/32, AM25 and two CR10s; Campbell Scientific).

Data gap filling

We used eddy flux and meteorological data measured over 10 yr, which included periods of instrument failures that required data gap filling for estimating daily and annual-scale carbon, water, and energy budgets. We tested the commonly applied algorithm for NEE gap filling and for carbon flux partitioning into ecosystem respiration (R_e) and GPP (Reichstein *et al.*, 2005; http://www.bgc-jena.mpg.de/~MDIwork/eddyproc/), but found that for the Yatir forest our own site-specific algorithm was more suitable (Afik, 2009). Briefly, missing NEE values (including the NEE night values when the wind friction velocity, U^*, was below a critical value, U_{crit}; Burba, 2013) were filled in with a three-step algorithm: (1) missing NEE values were replaced by average NEE values for the same time (± 0.5 h) of the days before and after the day with the missing value, using the neighboring 2, 5 or 8 d if needed in order to make sure that > 20% of data were available both before and after the gap; (2) for the rare occasions where a larger number of days (n) with gaps remained, the values for the same time (± 1.5 h instead of 0.5 h) from $n/2$ (if $n < 8$) or n d (if $n > 8$) before and after the gap were used the same way as in (1); (3) when larger gaps remained, the overall mean for the given hour measured within 30 d of the gap in the active season (November–April), and within 60 d in the nonactive season (summer), was used.

After gap filling, daytime ecosystem respiration ($R_{e\text{-}d}$, in μmol m^{-2} s^{-1}) was estimated based on measured night-time (i.e. when the global radiation was < 5 Wm^{-2}) values ($R_{e\text{-}n}$), averaged for the first three half-hours of each night. The daytime respiration for each half-hour was calculated according to Eqn 3 (Maseyk *et al.*, 2008b; Afik, 2009):

$$R_{e-d} = R_{e-n} \cdot (\alpha_1 \beta_s^{dT_s} + \alpha_2 \beta_w^{dT_a} + \alpha_3 \beta_f^{dT_a}) \qquad \text{Eqn 3}$$

where β_s, β_w and β_f are coefficients that correspond to soil, wood and foliage, respectively, dT_s and dT_a are soil and air temperature deviations from the values at the beginning of the night, and α_1, α_2 and α_3 are partitioning coefficients fixed at 0.5, 0.1 and 0.4, respectively. The β_s, β_w, and β_f coefficients were calculated as follows: $\beta_s = 2.45$ for wet soil (soil water content in the upper 30 cm above 20% vol); $\beta_s = 1.18$ for dry soil (based on the Grünzweig *et al.*, 2009 study at the same site); $\beta_f = 3.15 - 0.036\,T_a$; and

$$\beta_w = 1.34 + 0.46 \cdot \exp\left(-0.5 \cdot \left(\frac{\mathrm{DoY} - 162}{66.1}\right)^2\right) \qquad \text{Eqn 4}$$

where DoY is the day of the hydrological year, starting from 1 October. Finally, GPP was calculated as GPP = NEE − R_e. Negative values of the NEE and GPP indicate that the ecosystem is a CO_2 sink.

In total, 82% and 36% of NEE values in the final dataset used for further analysis were original values in the daytime and night-time, respectively. During hamsin events, these values reached 88% and 43%, respectively. The high proportion of night gaps is the result of excluding NEE values under low U^*. In further analysis, only hamsin events with > 80% of original daytime values were used for statistics.

Detection of hamsin events

Hamsin events were detected using a custom-based method where the end of the event corresponded to the day when its maximum daily T and VPD exceeded the corresponding values for the following day by > 5°C and > 1100 Pa, respectively. More details on the method and its testing in comparison to other methods are provided in the Supporting Information Methods S1.

Statistics

The effect of a specific hamsin event on a variable X was evaluated by the relative span of X as follows:

$$r_X = \frac{\overline{(\overline{X_b}, \overline{X_a})} - \overline{X_h}}{\overline{X}}, \qquad \text{Eqn 5}$$

where $\overline{X}_b$, $\overline{X}_a$ and $\overline{X}_h$ are the mean daytime X values for the day before the hamsin, the day after the hamsin, and the days of the hamsin, respectively, and $\overline{X}$ is the overall daytime mean from the day before the hamsin to the day after the hamsin.

The soil moisture conditions were separated into three classes, depending on the soil moisture in the top 30 cm (soil water content (SWC), % vol): dry (SWC < 10%), medium (10 ≤ SWC < 20%) and moist (SWC ≥ 20%).

Results and Discussion

Changes in environmental variables during hamsins

Based on our 'end-of-hamsin' detection method applied to the site's 10 yr dataset (see Notes S1 and Table S1), hamsin events were most frequent during the period from February to June (Fig. 1). Following the precipitation maximum for the rainy season in January (Fig. 1), April was the peak frequency of hamsin events (three hamsin events per month on average for the study period), which, notably, coincided with the peak in photosynthetic activities for this ecosystem (Maseyk *et al.*, 2008a).

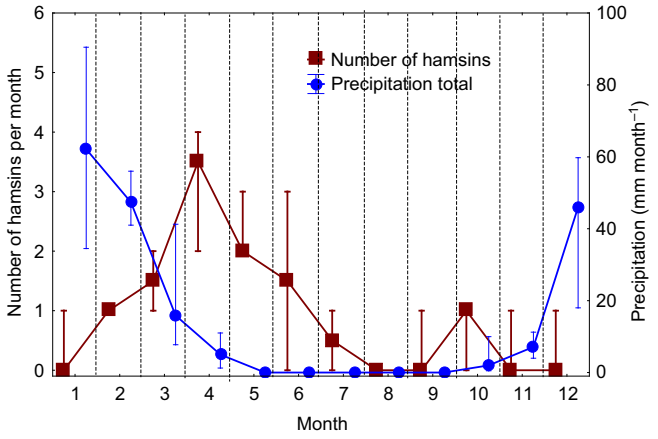

Fig. 1 Median monthly hamsin events (detected by the 'end-of-hamsin' method), and mean monthly precipitation for 2000–2010 (whiskers represent the 25–75% range).

Typically, the temperature and VPD increase during the onset of the event and then fall rapidly at the end of the event, with high night-time temperature (T_{air}) and VPD values (Fig. 2a,b for the wet and dry periods, respectively), which were typical for any season (Table 1). The mean daytime VPD increased compared with the day preceding the hamsin by 165% in dry conditions (SWC < 10%) and by over 240% in wetter conditions (SWC > 20%; Table 1), with the highest increase reaching 4400 Pa. In addition, the range of VPD variation during a hamsin event (calculated as the difference between the daytime mean VPD values during an event and the mean daytime VPD values a day before and a day after an event) varied from 1597 Pa (for SWC < 10%) to 1299 Pa (for SWC > 20%; see Table 1). Air temperature showed similar trends, with a temperature increase of over 10°C on an event basis in both the wet and dry season (Fig. 2a,b).

The incoming solar radiation (R_g) did not change significantly during hamsin events in the dry season, whereas in the wet season, R_g decreased considerably after hamsin events. Simultaneously, the proportion of diffuse radiation increased considerably during, and even more so after, hamsin events (Table 1). This result was probably because the hamsin is usually associated with a cloudless sky but also includes increased dust from the Arabian Peninsula. Following hamsin events, the cloudiness often increases, which is associated with the decreased R_g but also with the high diffuse radiation. However, the radiation characteristics described earlier were average responses, and clear skies and reduced diffuse radiation were also observed following hamsin events.

Ecosystem response to hamsin events

Daytime NEE decreased (i.e. became less negative; with somewhat increased, more positive, night-time R_e) during the hamsin events and then fully recovered to pre-event values within the first day following the end of the event, in both the rainy and dry seasons (Figs 2e and f for the wet and dry periods, respectively; see also Table 1). In relative terms, daytime NEE decreased to 75%, 45% and 0% of its pre-event values with decreasing SWC during the drying season (for SWC > 20%, in the range 10–20% and < 10%, respectively; Table 1), but the prehamsin NEE fluxes also decreased by *c.* 90% for the same SWC intervals, from −9.2 to −1.1 μmol m^{-2} s^{-1}. Following the hamsin events, full recovery to pre-event values was observed for NEE in the high and intermediate SWC conditions. It was also observed in the low SWC conditions for which fluxes were in general very low. Similar results were obtained for GPP. Full recovery of GPP to pre-event values was also observed immediately following the hamsin, often with some enhancement relatively to prehamsin values in the driest conditions.

During hamsin events, both NEE and GPP were linearly correlated with VPD, the dominant variable during such events, with an overall R^2 ranging between 0.2 and 0.8 for individual hamsin events, with the lower values mainly from low flux summer periods (Table 2; see a typical example in Fig. 3b). While the low fluxes in the dry period make it more difficult to assess ecosystem response, the effects of VPD are still apparent, for example on GPP and g_c (Fig. 3b,e), although with different sensitivities, as discussed in the following section. Note also that, generally, canopy scale flux measurements show considerable greater variation than other meteorological measurements (e.g. VPD), somewhat reducing R^2 values, especially when these fluxes are low. Nonetheless, linear relationships improved when a higher solar radiation threshold was used, that is, using midday values only. For example, applying a threshold of $R_g > 400$ W m^{-2} resulted in R^2 values for NEE or GPP vs VPD that increased from *c.* 0.4 to 0.7 and 0.6, respectively. This is because daily transition periods with low fluxes and variable light conditions (morning and evening) show the largest deviations from the regression lines in the parameters considered.

The canopy conductance, g_c, showed, on average, a strong reduction during hamsin events (down to 17% of the pre-event in the high SWC conditions; Table 1), and a clear response to VPD in both the wet and dry seasons (Fig. 3e), but also a fast recovery following the events. Note, however, that g_c depends on VPD (Eqn 1), mediated by Q, and therefore reflects a complex response to changes in the physical environment and physiological response. Recovery (and even enhancement) of g_c was observed at all SWC values after the hamsin events, with values between 131% and 141% of prehamsin values. This is probably because VPD after the hamsin event was usually lower than before the event (Table 1).

The water fluxes showed a weak and variable response to the hamsin conditions. Indeed, the relative change in ET during a hamsin event (Fig. 4) was, on average, one-third of that for GPP. Daily ET and Q values showed some increase under high SWC conditions and no, or a small, decrease under the drier conditions. Similarly, the diurnal courses of both ET and Q did not usually change markedly during hamsins (Fig. 2g,h; Table 1). However, in the spring, ET often decreased considerably following a hamsin event (Fig. 1g), which was probably associated with the dramatic decrease in VPD and air temperature at the end of the hamsin events, occasionally accompanied by rainfall. Notably, changes in SWC at 5, 15 and 30 cm (Fig. 1c,d) during

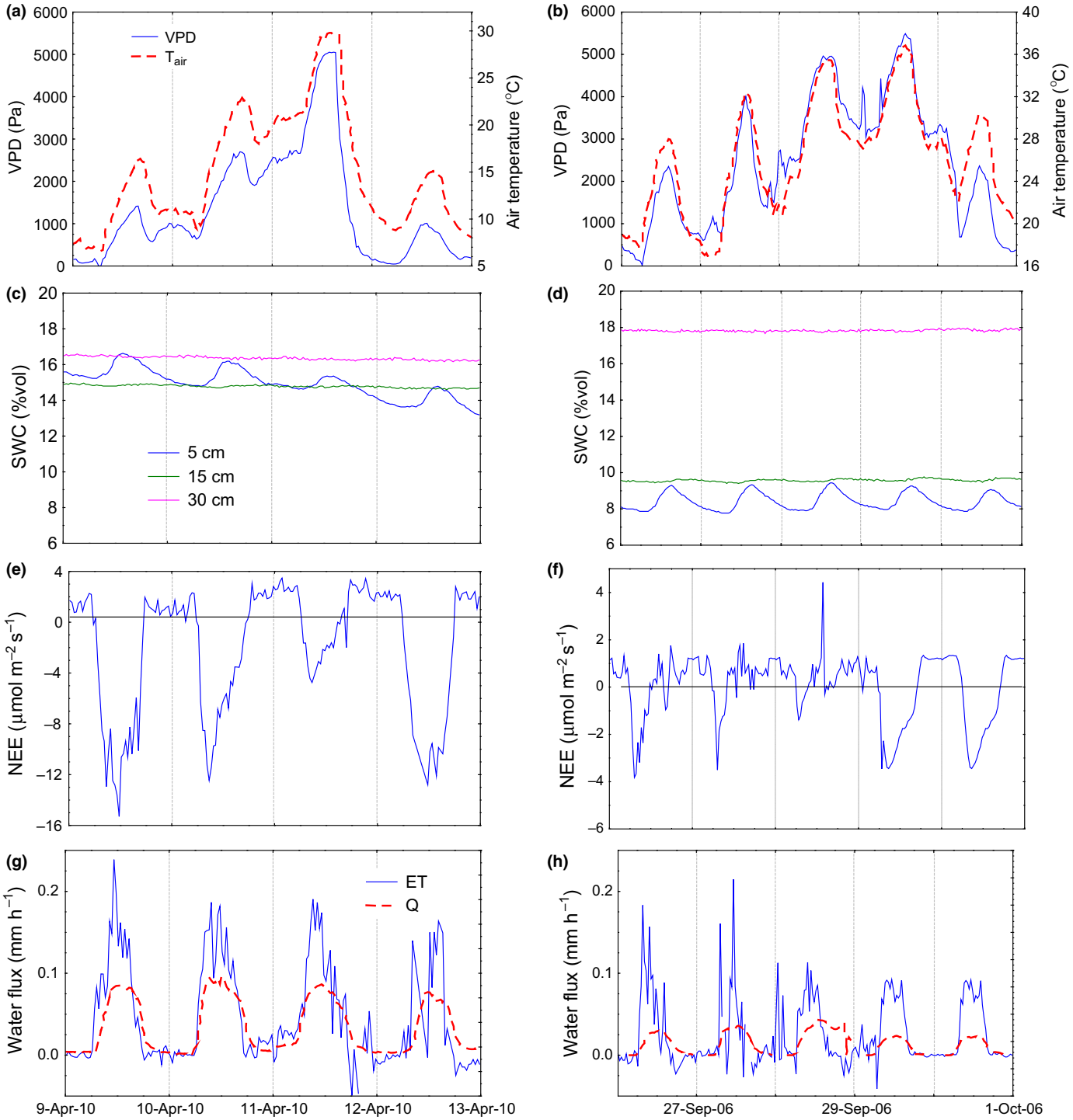

Fig. 2 Typical behavior of climatic and ecosystem variables during 2 d of a hamsin event in the spring (a, c, e, g) and during a 3 d event in the summer (b, d, f, h). Note the different scales in (e) and (f). SWC, soil water content; Q, rate of sap flow; VPD, vapor pressure deficit; NEE, net ecosystem carbon exchange; ET, evapotranspiration.

hamsin periods were negligible. Changes in the SWC were detected only in the top 5 cm layer, which reflected day to night changes, and the overall reduction in the volumetric SWC in this layer through 4 d of a hamsin was only *c.* 2% in the wet season.

The weak response of the water fluxes to hamsin events probably reflected a tight balance between the effects of the increasing VPD and decreasing stomatal (and canopy) conductance. Indeed, the large increases in VPD during hamsin events were compensated by a marked decrease in g_c values (related to a decrease in the atmosphere to leaf CO_2 flux and in the GPP). Accordingly, the dependence of ET and Q on the VPD was associated with low R^2 values, < 0.1 for 84% of events (Fig. 3c; Table 2). The

Table 1 Observed daytime average meteorological and gas exchange variables during hamsin events under different soil moisture conditions (midday means are for daytime when incoming $R_g > 200\ W\ m^{-2}$)

SWC (%vol)	≤10			(10–20)			>20		
Hamsin events	39			62			25		
	Before hamsin	During hamsin	After hamsin	Before hamsin	During hamsin	After hamsin	Before hamsin	During hamsin	After hamsin
VPD (Pa)	**2068**	**3416 (165)**	**1571 (76)**	**1471**	**2871 (195)**	**1154 (78)**	**858**	**2065 (241)**	**674 (79)**
Air temperature (°C)	**23.9**	**28.6 (120)**	**23.2 (97)**	**18.5**	**25.1 (136)**	**18.1 (98)**	**14.3**	**20.2 (141)**	**14.1 (99)**
R_g (W m^{-2})	**671.8**	667.7 (99)	661.8 (99)	**634.4**	**609.5 (96)**	**583.2 (92)**	**558.7**	**573.3 (103)**	**454.8 (81)**
% of diffuse radiation	**21.3**	**27.6 (130)**	**30.8 (145)**	**32.9**	**38.2 (116)**	**48.5 (148)**	**37.7**	**29.6 (79)**	**69.3 (184)**
NEE (μmol m^{-2} s^{-1})	**−1.06**	**−0.00 (0)**	**−1.44 (137)**	**−5.14**	**−2.29 (45)**	**−5.85 (114)**	**−9.26**	**−6.97 (75)**	**−9.46 (102)**
GPP (μmol m^{-2} s^{-1})	**2.10**	**1.19 (57)**	**2.88 (137)**	**6.98**	**4.45 (64)**	**7.76 (111)**	**11.10**	**9.43 (85)**	**12.07 (109)**
ET (mm d^{-1})	**1.22**	**0.98 (80)**	**1.17 (96)**	2.32	2.16 (93)	2.05 (88)	**3.48**	**4.09 (118)**	**3.04 (87)**
Q (mm d^{-1})	0.60	0.56 (**93**)	0.48 (80)	1.20	1.22 (102)	1.17 (98)	1.93	2.12 (110)	1.77 (92)
Canopy conductance, g_c (mm d^{-1})	**7.2**	**4.1 (58)**	**9.6 (134)**	24.1	11.7 (49)	31.4 (131)	53.2	20.8 (39)	78.3 (147)
Water-use efficiency, W (g C kg^{-1} H_2O)	4.5	3.5 (77)	6.2 (138)	**6.7**	**4.5 (68)**	**7.7 (115)**	20.1	10.5 (52)	6.4 (32)
Intrinsic water-use efficiency, W_i (g C kg^{-1} H_2O kPa)	10.8	11.3 (104)	10.9 (101)	**10.0**	**14.9 (150)**	**10.3 (103)**	18.1	21.5 (119)	4.1 (23)

Values of canopy conductance (g_c), water-use efficiency (W) and intrinsic water-use efficiency (W_i) are calculated on a daily basis. Values in parentheses represent percentage of prehamsin values. Data with a statistically significant effect of hamsin ($P < 0.05$) are shown in bold.
VPD, vapor pressure deficit; R_g, incoming global radiation; NEE, net ecosystem carbon exchange; GPP, gross primary productivity; ET, evapotranspiration; Q, stand sap flow.

Table 2 Mean slopes and correlation coefficients (R^2, in parentheses) of linear regression of flux variables on vapor pressure deficit (VPD) for different soil moisture contents in the upper 30 cm

	SWC span (%vol)		
Regression slopes d/dVPD	>20	10–20	≤10
NEE (μmol m^{-2} s^{-1} kPa^{-1})	2.71 (0.48)	2.09 (0.60)	1.32 (0.55)
GPP (μmol m^{-2} s^{-1} kPa^{-1})	2.84 (0.44)	2.02 (0.58)	1.28 (0.59)
ET (mm h^{-1} kPa^{-1})	0.059 (0.28)	0.016 (0.13)	−0.028 (0.21)
Q (mm h^{-1} kPa^{-1})	0.020 (0.33)	0.007 (0.21)	0.004 (0.20)
g_c (mm h^{-1} kPa^{-1})	−14.03 (0.64)	−8.74 (0.82)	−2.55 (0.86)
W (g C kg H_2O^{-1} kPa^{-1})	−11.73 (0.58)	−2.95 (0.56)	−2.17 (0.60)
W_i (g C kg H_2O^{-1})	−0.78 (0.65)	3.26 (0.66)	−0.01 (0.50)

Regressions were calculated for daytime ($R_g > 200\ W\ m^{-2}$) data of individual hamsin events using half-hourly values for net ecosystem carbon exchange (NEE), gross primary productivity (GPP), evapotranspiration (ET) and stand sap flow (Q) and on a daily basis for water-use efficiency (W), canopy conductance (g_c) and intrinsic water-use efficiency (W_i). The day before and the day after hamsin events are included in the regression. For the NEE and GPP, only data with R^2 values of linear dependencies on VPD above 0.4 were used (53% and 46% of hamsin events, respectively). For ET and Q, the corresponding R^2 threshold was 0.1 (15% and 55% of hamsin events with the available data, respectively).

only exceptions were spring hamsin events, where R^2 for the ET-VPD regressions reached 0.35–0.40. Such cases may occur mostly under high SWC, when soil evaporation, directly depending on VPD, represents a considerable proportion of ET.

The tradeoff between the increasing VPD and leaf conductance was also reflected in the W and W_i values. W decreased, on average, during the hamsin events under all SWC conditions, which could be expected because of the decrease in carbon fluxes with little change in water fluxes (Table 1). The full recovery of W to pre-event values was observed on the first day following the hamsin in the intermediate and low SWC conditions, but not in the high SWC conditions. Note, however, that the data were highly variable, and the changes were significant only in the intermediate SWC conditions (Table 1).

Changes in W_i could also be expected, as the relative change in g_c was generally greater than for GPP (see Table 1), which could lead to an increase in W_i. Indeed, W_i values showed a strong increase during hamsin in the intermediate SWC range, a lower increase at high SWC, but little change in the driest conditions (Table 1). Such variations in W_i values reflect a differential response to heat waves between canopy conductance and carbon fluxes, associated with the sensitivity of the carbon fluxes to factors other than g_c (e.g. light, temperature, metabolic signals). Generally, on daily to annual timescales, GPP tended to remain proportional to transpiration, which resulted in a relatively constant W and W_i on these timescales (Law *et al.*, 2000, 2002). However, other studies, particularly those that examined Mediterranean ecosystems, also reported a decrease in W under low SWC (Reichstein *et al.*, 2002) or high VPD (Moriana *et al.*, 2002).

Differential response to air and soil moisture

The intense but short-term changes during hamsin events (Fig. 1) involved large changes in atmospheric parameters, such as VPD,

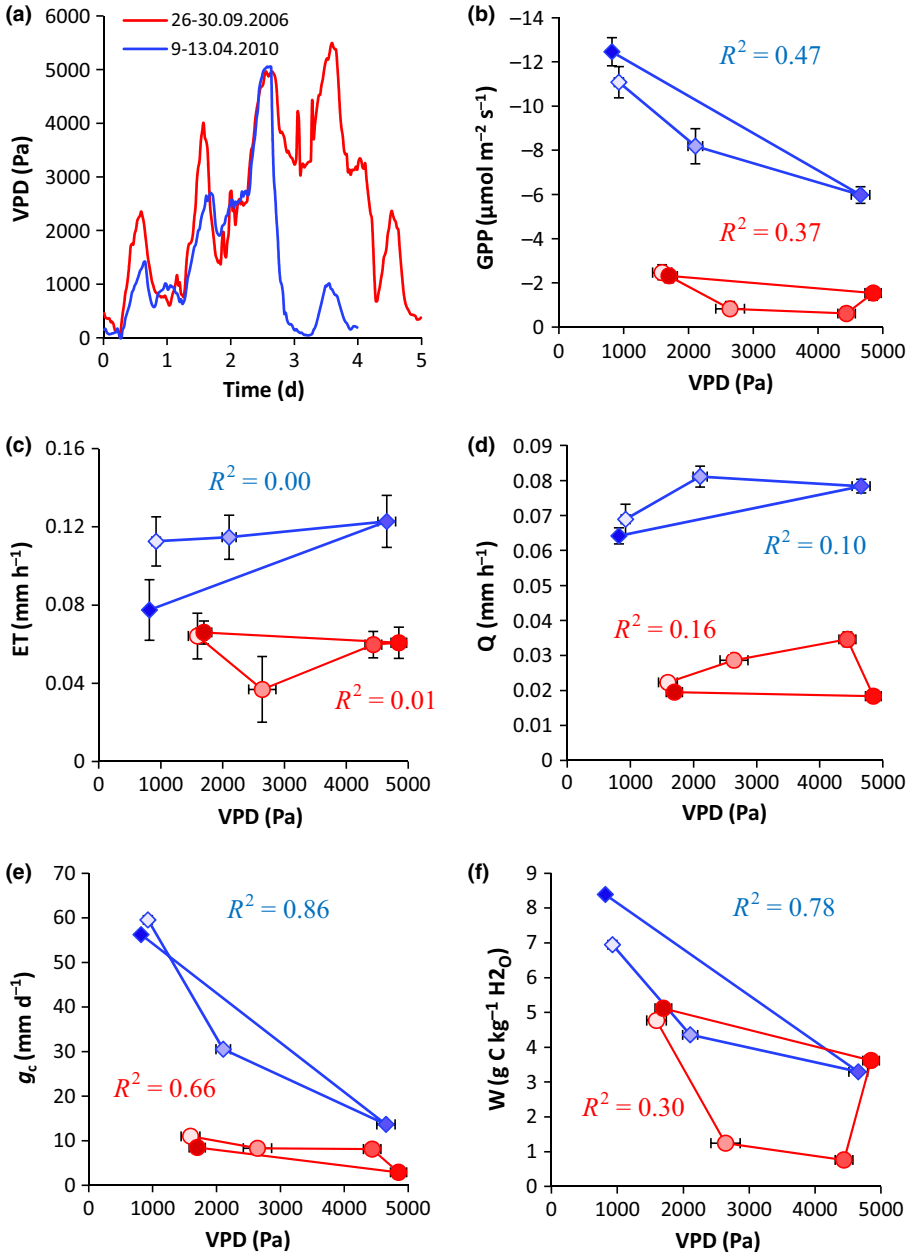

Fig. 3 Changes in vapor pressure deficit (VPD) during hamsin events (a; *x*-axis includes the day before and after the event), and examples of the dependence on VPD of observed daytime ($R_g > 200$ W m^{-2}) values of ecosystem variables during spring (blue lines and symbols) and summer (red lines and symbols) hamsin events (b–f). GPP, gross primary productivity; ET, evapotranspiration; *Q*, sap flow; g_c, canopy conductance; *W*, water-use efficiency. Darker points on (b–f) correspond to later days. R^2 values on the graphs are calculated on a half-hourly base.

but negligible changes in soil moisture content on the relevant timescale (few days). However, the occurrence of hamsin events throughout the seasonal drying period at different SWC values provided the opportunity to examine the interactions of the atmospheric (VPD) and soil (SWC) factors on limiting ecosystem activities on the longer timescale (seasonal).

A decrease in the sensitivity of ecosystem variables to VPD as soil dries up has been reported previously(Oren *et al.*, 1999; Addington *et al.*, 2004; Gu *et al.*, 2006; Maseyk, 2006). Here, we examine the interactions of VPD and SWC as reflected in the dependence of the slopes of the linear best-fit lines of d*X*/dVPD on soil moisture, (where *X* is a specific ecosystem variable; Fig. 5). The observed dNEE/dVPD and dGPP/dVPD showed direct dependence on soil moisture (Fig. 5a,b), with decreasing sensitivity (decreasing slope) of dNEE/dVPD and dGPP/dVPD with decreasing soil moisture (relatively low R^2 values reflect the relatively small fluxes and their sensitivity to a wide range of factors). This dependence was stronger for SWC at the depths of 5 and 15 cm than for SWC at 30 cm (only data for 15 cm are shown). These observations clearly demonstrated that as the soil dries out, soil moisture availability becomes the dominant factor, over VPD, in limiting ecosystem activities, with most functions ultimately becoming insensitive to VPD.

The interactions of the water fluxes, ET and T_r, with VPD and SWC were more complex. As noted earlier, under high soil moisture conditions, ET reflects the effects of VPD on soil evaporation. This can explain the observations reported in Fig. 5(d), showing increased sensitivity of ET to VPD with increasing soil moisture. By contrast, T_r, represented by measured sap flow, is influenced by the interactions of g_c and VPD noted earlier.

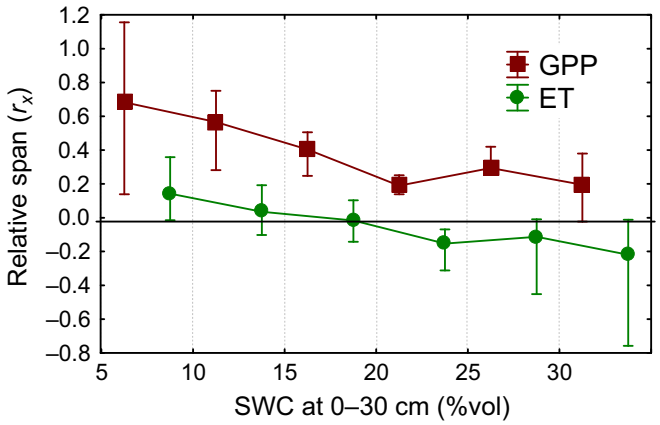

Fig. 4 Dependence of the relative span of observed daytime gross primary productivity (GPP) and evapotranspiration (ET) during hamsin development (see Eqn 5) on soil moisture for the entire period of observation (medians per soil water content (SWC) interval; error bars represent quartiles). A negative span indicates that mean values under the hamsin are higher than those before and after the event.

Consequently, the dQ/dVPD slope was generally lower than dET/dVPD, as well as its response to soil moisture (Fig. 5c). Sap flow exhibited a weak response to VPD on a daily timescale (Fig. 6a), but a strong bimodal response to changes in SWC (Fig. 6b). As expected, daily sap flow increased with water availability, but only up to about an SWC of 22%. Under conditions of SWC > 22%, corresponding to the wet season and characterized by more cloudy weather, sap flow exhibited a negative response to an increase in SWC (Fig. 6b). This is explained by the effects of the decreasing light intensity on stomatal conductance and g_c. This is consistent with the general correlation between transpiration and GPP under nonstressed conditions. GPP at our site had already been shown to be light-dependent, with the light saturation at photosynthetically active radiation > 1200 μmol m^{-2} s^{-1} (Maseyk *et al.*, 2008a). Indeed, the correlation coefficient between daily sap flow values and net radiation was 0.21 for SWC < 22% in the summer, when saturating light intensity prevailed, but increased to 0.60 for SWC ≥ 22% in the winter, when light intensities were much lower and variable.

Note that on the seasonal timescale, the same range of VPD values could have very different effects on ecosystem activities, supporting the idea that the effect of SWC shown in Fig. 5 is not simply a consequence of the possible correlation between SWC and VPD (i.e. dry conditions associated with high VPD and vice versa).

Based on these results, we concluded that on daily to seasonal timescales, changes in daily transpiration were strongly (and almost exclusively) dominated by soil moisture availability. The interactions of Q or T_r with VPD were apparently important primarily on the short, hourly, timescales (not shown), consistent with the idea that stomata optimize the time and extent of carbon uptake with respect to light and VPD, while preventing water stress damage.

Interactions between air and soil moisture effects on ecosystem activities were also noted recently in an irrigation study conducted in a semiarid ponderosa pine stand (Ruehr *et al.*, 2014). This study showed a strong correlation between midday sap flow and soil moisture, independent of VPD, and a strong dependence of canopy conductance on both soil moisture and VPD. Both of these results were consistent with our observations. These authors also found that GPP and NEE were influenced both by summer temperatures and VPD (−17% and −38%, respectively) and by a reduction in summer precipitation (−9% and −85%, respectively), indicating strong interacting effects of both atmospheric (VPD) and soil (precipitation) factors. Our results, although qualitatively similar, may not be quantitatively comparable to this other study because of the large differences in experimental setup and climatic conditions between the two ecosystems.

Prediction of NEE based on hamsin data

The combination of a strong ecosystem response to large changes in the environmental conditions and the fast and full reversibility of the response offers an unusual testbed for developing predictive algorithms. Based on the dependence of the ecosystem fluxes on VPD and the flux sensitivity to seasonal changes in the SWC, we tested our ability to forecast NEE over the annual cycle. We performed regression analysis of NEE using two equations as follows:

$$\mathrm{NEE} = (a_1 + b_1\mathrm{SWC}) + (a_2 + b_2\mathrm{SWC}) \cdot \mathrm{VPD}, \qquad \text{Eqn 6}$$

and

$$\mathrm{NEE} = [(a_1 + b_1\mathrm{SWC}) + (a_2 + b_2\mathrm{SWC}) \cdot \mathrm{VPD}] \cdot [1 - \exp(-b_3(R_g - c))]. \qquad \text{Eqn 7}$$

Eqn 6 was applied only to the midday values (R_g > 200 W m^{-2}) to minimize the effects of large variations in radiation. Eqn 7 was applied to the entire daytime period (R_g > 5 W m^{-2}) and also accounted for the NEE light response curve (last term of the equation). Each equation was applied both to the entire data set for the 10 yr study period and to the hamsin events only during that same period.

Eqn 6 yielded a linear correlation between the measured and predicted NEE values, with R^2 values of 0.60 and 0.59 for the entire data set and for the hamsin days only, respectively. Using Eqn 7, the regressions yielded higher R^2 values of 0.67 and 0.65 for the hamsin days and the entire dataset, respectively (possibly as a result of better accounting for diurnal cycle effects). We then used the fitted parameters for Eqns 6 and 7 that were obtained for the hamsin days only to test the NEE forecast capabilities across the entire data set. Using Eqn 7, the prediction based on the parameters from the hamsin days only resulted in an almost identical correlation coefficient to that obtained when using the fitted parameters on the entire data set. In both cases, the predicted NEE values were within the range of the observed values (not shown). These results suggest that the response mechanisms to the short-term heat waves are not different from the general response to seasonal and interannual variations in the local semiarid environmental conditions. The results also indicate that the short-term hamsin events could represent the range of

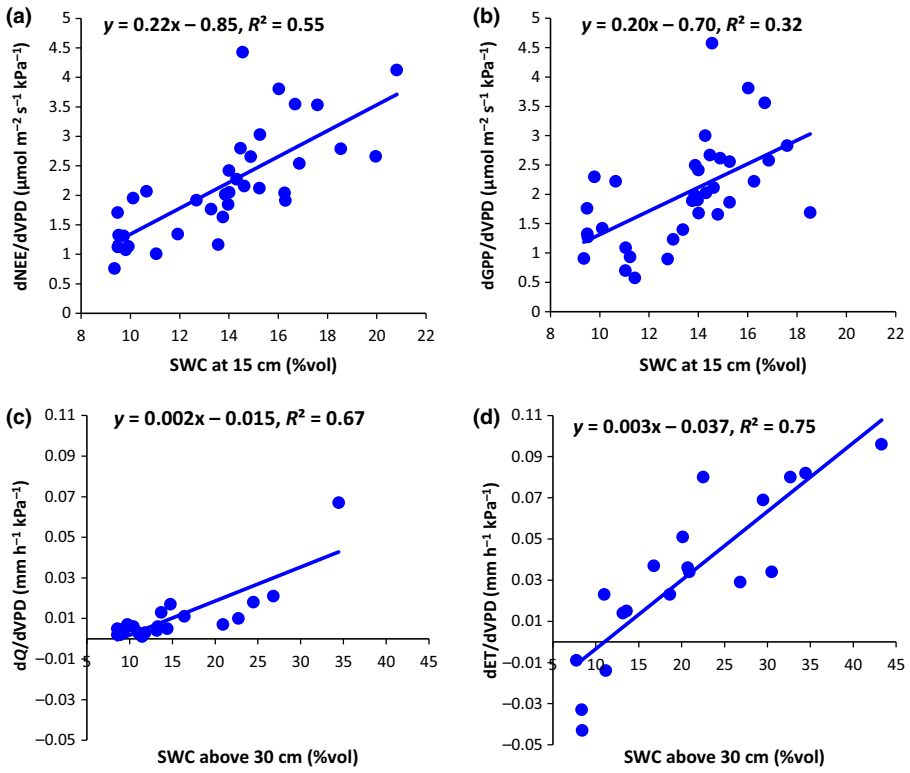

Fig. 5 Dependence of net ecosystem carbon exchange (NEE; a), gross primary productivity (GPP; b), sap flow (Q; c), and evapotranspiration (ET; d) sensitivity to vapor pressure deficit (VPD) (slope of linear correlation) on the soil water content (SWC) at different depths (depths with the best dependence were selected) along the seasonal cycle. All slopes were calculated for daytime values ($R_g > 200\ W\ m^{-2}$). For the NEE and GPP, only data with R^2 values for corresponding dependences on VPD above 0.4 were used (53% and 46% of hamsin events, respectively). For ET and Q, the R^2 threshold was 0.1 (55% of hamsin events with the available data).

environmental variations that would otherwise require a much longer observation period.

Effects of hamsins on annual NEE

The strong reduction in carbon uptake (NEE or GPP; Fig. 1) during hamsin events, combined with the high frequency of such events at the peak activity period (Fig. 2) implies that the frequency and intensity of the events could significantly influence the annual productivity of the forest. By contrast, the high degree of resilience greatly reduces the extent of the hamsin effects and allows maximum productivity (NEE), even when intervals between events are short.

To assess the combined effects of heat waves and resilience on the annual carbon budget of the forest, the relative difference between the actual mean annual NEE was compared with the mean NEE assuming that no hamsin events had occurred, according to:

$$\alpha = \frac{(\mathrm{NEE} - \mathrm{NEE}^*)}{\mathrm{NEE}^*} \qquad \text{Eqn 8}$$

NEE* and NEE are the annual net CO_2 exchange flux excluding or including hamsin days, respectively, where: $\mathrm{NEE}^* = \overline{F}_{\mathrm{no\,hamsin}} \cdot (N_{\mathrm{hamsin}} + N_{\mathrm{no\,hamsin}})$; and $\mathrm{NEE} = \overline{F}_{\mathrm{no\,hamsin}} \cdot N_{\mathrm{no\,hamsin}} + \overline{F}_{\mathrm{hamsin}} \cdot N_{\mathrm{hamsin}}$ and where N and $\overline{F}$ are the number of days yr^{-1} and the mean daily net CO_2 flux (during hamsin or not, as indicated), respectively. The effects on the GPP were estimated in a similar way.

This analysis indicated that annual average NEE and GPP during the study period were reduced by the hamsin events by 15.4% and 4.2%, respectively (in total, hamsin days constituted 10.4% of the study period). Note, however, that for the average NEE and GPP fluxes of −44.4 and −159.1 mmol $m^{-2}\,d^{-1}$, respectively, the percentage differences translate to a similar quantity of 6.8 and 6.7 mmol $m^{-2}\,d^{-1}$. Remembering that $\mathrm{NEE} = \mathrm{GPP} + R_e$, the results indicate that, on average, hamsin events influenced predominantly GPP, the leaf photosynthetic CO_2 flux. The proportionally large effects on NEE reflect the fact that it is a small residual flux of two large opposing fluxes of GPP and R_e and, accordingly, annual R_e did not change significantly as a result of hamsin effects (annual average R_e was 115 mmol $m^{-2}\,d^{-1}$, both including and excluding hamsin events). Finally, we note that the annual-scale analysis can also be used to assess the importance of the resilience component. For example, extending hamsin events by 3 d on average during the wet season (February–May) would decrease annual NEE by *c.* 28% compared with the no-hamsin scenario (with a smaller effect during summer when fluxes are small).

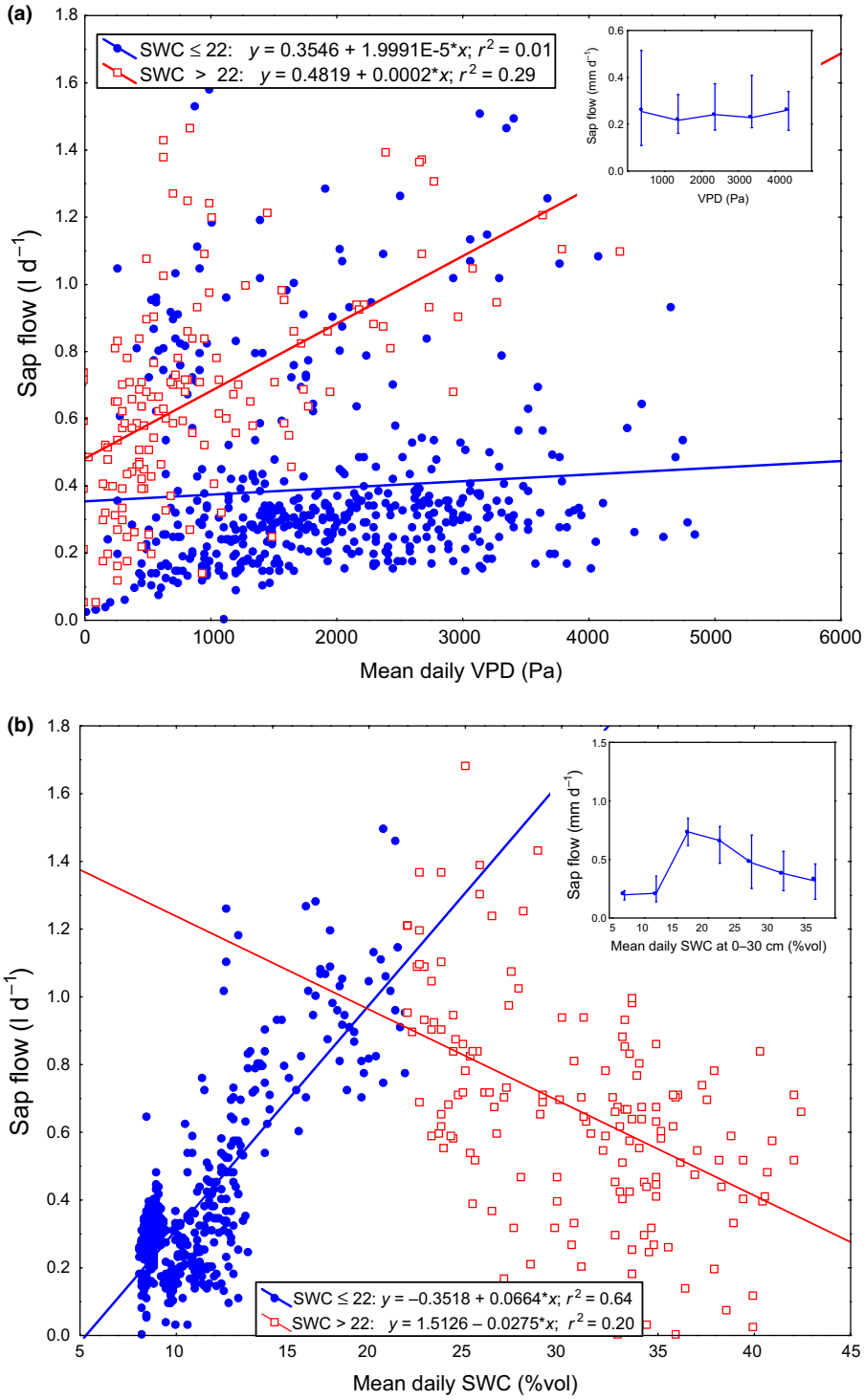

Fig. 6 Dependence of measured sap flow daily totals on mean daily vapor pressure deficit (VPD) (a) and soil water content (SWC) at 0–30 cm, separately for SWC < 22% and SWC ≥ 22%, in the upper layer (b), for the study period 2001–2010. The inserts represent medians and quartiles of sap flow daily totals by VPD (a) and SWC (b) classes.

It is generally accepted that major episodic heat waves in temperate regions lead to large decreases in ecosystem productivity (Baldocchi, 1997; Ciais *et al.*, 2005; Reichstein *et al.*, 2013). Furthermore, after droughts, forests often require long recovery periods (from months to several years). In particular, heat waves and droughts can result in irreversible photoinhibition, mortality of foliage, branches or entire trees, and enhanced pest attacks, among other types of damage to the forest (Brodribb, 1996; Reichstein *et al.*, 2013; Saatchi *et al.*, 2013), including irreversible changes in forest composition (Cavin *et al.*, 2013). Our results have shown that in the case of the pine ecosystem adapted to semiarid conditions (Weinstein, 1989; Rotenberg & Yakir, 2010; Schiller, 2011), a high degree of resilience was achieved, with rapid full recovery and no irreversible damage associated with the short but intense heat wave events, with the highest frequency during the short peak activity period. We suggest that this

resilience is probably a key to the survival and productivity of the forest in a harsh environment, which may become the prevalent environment in many currently wetter regions. The results of this study also demonstrate the utility of short-term heat waves in studying the response of forest ecosystems to stress and in separating the effects of atmospheric (VPD and temperature) factors from those of the soil (SWC).

Acknowledgements

Different parts of this long-term work were supported by KKL-JNF, The Cathy Wills and Robert Lewis Program in Environmental Science, the Israel Science Foundation (ISF), the Israeli Water Authority, and the High Council for Scientific and Technological Cooperation between France and Israel (contract ref. 09 F2/ENERGY). The authors thank Drs Shabtai Cohen and Gabriel Schiller from the ARO Volcani Center, Israel, for providing early period sap flow data, and Tal Kaneti for assistance in sap flow sensor manufacturing.

Author contributions

D.Y., E.R., T.K. and K.M. planned and designed the research; E.R. was responsible for eddy covariance data, T.K. for sap-flow data, K.M. for physiological data, and J.O. supplied supporting model simulation. F.T. performed data analysis and wrote the first draft of the manuscript, which was revised and expanded by all co-authors.

References

Addington RN, Mitchell RJ, Oren R, Donovan LA. 2004. Stomatal sensitivity to vapor pressure deficit and its relationship to hydraulic conductance in *Pinus palustris*. *Tree Physiology* **24**: 561–569.

Afik T. 2009. *Quantitative estimation of CO_2 fluxes in a semi-arid forest and their dependence on climatic factors*. Thesis submitted to R.H. Smith Faculty of Agriculture, Food and Environment of Hebrew University, Rehovot, Israel (in Hebrew).

Allen CD, Macalady AK, Chenchouni H, Bachelet D, McDowell N, Vennetier M, Kitzberger T, Rigling A, Breshears DD, Hogg EH *et al.* 2010. A global overview of drought and heat-induced tree mortality reveals emerging climate change risks for forests. *Forest Ecology and Management* **259**: 660–684.

Aubinet M, Grelle A, Ibrom A, Rannik U, Moncrieff J, Foken T, Kowalski AS, Martin PH, Berbigier P, Bernhofer Ch *et al.* 2000. Estimates of the annual net carbon and water exchange of European forests: the EUROFLUX methodology. *Advances in Ecological Research* **30**: 113–175.

Baldocchi D. 1997. Measuring and modeling carbon dioxide and water vapour exchange over a temperate broad-leaved forest during the 1995 summer drought. *Plant, Cell & Environment* **20**: 1108–1122.

Beer C, Ciais P, Reichstein M, Baldocchi D, Law BE, Papale D, Soussana J-F, Ammann C, Buchmann N, Frank D *et al.* 2009. Temporal and among-site variability of inherent water use efficiency at the ecosystem level. *Global Biogeochemical Cycles* **23**: GB2018.

Bonan G. 2008. Forests and climate change: forcings, feedbacks, and the climate benefits of forests. *Science* **320**: 1444–1449.

Breda N, Badeau V. 2008. Forest tree responses to extreme drought and some biotic events: towards a selection according to hazard tolerance? *Comptes Rendus Geoscience* **340**: 651–662.

Brodribb T. 1996. Dynamics of changing intercellular CO_2 concentration (c_i) during drought and determination of minimum functional c_i. *Plant Physiology* **111**: 179–185.

Burba G. 2013. *Eddy covariance method for scientific, industrial, agricultural, and regulatory applications*. Lincoln, NE, USA: LI-COR Biosciences.

Cavin L, Mountford EP, Peterken GF, Jump AS. 2013. Extreme drought alters competitive dominance within and between tree species in a mixed forest stand. *Functional Ecology* **27**: 1424–1435.

Cermak J, Kucera J, Nadezhdina N. 2004. Sap flow measurements with some thermodynamic methods, flow integration within trees and scaling up from sample trees to entire forest stands. *Trees* **18**: 529–546.

Ciais P, Reichstein M, Viovy N, Granier A, Ogee J, Allard V, Aubinet M, Buchmann N, Bernhofer C, Carrara A *et al.* 2005. Europe-wide reduction in primary productivity caused by the heat and drought in 2003. *Nature* **437**: 529–533.

Farquhar GD, Ehleringer JR, Hubick KT. 1989. Carbon-isotope discrimination and photosynthesis. *Annual Review of Plant Physiology and Plant Molecular Biology* **40**: 503–507.

Gat Z. 1990. The regime of spring sharavs in Israel. *Meteorologia be Israel* **90/1–2**: 24–25.

Girard F, Vennetier M, Guibal F, Corona C, Ouarmim S, Herrero A. 2012. *Pinus halepensis* Mill. crown development and fruiting declined with repeated drought in Mediterranean France. *European Journal of Forest Research* **131**: 919–931.

Göckede M, Foken T, Aubinet M, Aurela M, Banza J, Bernhofer C, Bonnefond JM, Brunet Y, Carrara A, Clement R *et al.* 2008. Quality control of CarboEurope fluxdata – part 1: coupling footprint analyses with flux data qualityassessment to evaluate sites in forest ecosystems. *Biogeosciences* **5**: 433–450.

Goldammer JG. 2010. *Preliminary assessment of the fire situation in Western Russia. GFMC*. [WWW document] URL http://www.fire.uni-freiburg.de/intro/about4_2010-Dateien/GFMC-RUS-State-DUMA-18-September-2010-Fire-Report.pdf [accessed 15 August 2010].

Goldreich Y. 2003. *The climate of Israel. Observation, research and application*. New York, NY, USA: Kluwer Academic/Plenum Pub.

Granier A. 1985. Une nouvelle méthode pour la mesure du fluxdesève brute dans le tronc des arbres. *Annales des Sciences Forestieres* **42**: 193–200.

Grünzweig JM, Gelfand I, Fried Y, Yakir D. 2007. Biogeochemical factors contributing to enhanced carbon storage following afforestation of a semi-arid shrubland. *Biogeosciences* **4**: 891–904.

Grünzweig JM, Hemming D, Maseyk K, Lin T, Rotenberg E, Raz-Yaseef N, Falloon PD, Yakir D. 2009. Water limitation to soil CO_2 efflux in a pine forest at the semiarid "timberline". *Journal of Geophysical Research: Biogeosciences* **114**: G03008.

Gu L, Meyers T, Pallardy SG, Hanson PJ, Yang B, Heuer M, Hosman KP, Riggs JS, Sluss D, Wullschleger SD. 2006. Direct and indirect effects of atmospheric conditions and soil moisture on surface energy partitioning revealed by a prolonged drought at a temperate forest site. *Journal of Geophysical Research* **111**: D16102.

Keenan TF, Hollinger DY, Bohrer G, Dragoni D, Munger JW, Schmid HP, Richardson AD. 2013. Increase in forest water-use efficiency as atmospheric carbon dioxide concentrations rise. *Nature* **499**: 324–328.

Klein T, Di Matteo G, Rotenberg E, Cohen S, Yakir D. 2013. Differential ecophysiological response of a major Mediterranean pine species across a climatic gradient. *Tree Physiology* **33**: 26–36.

Klein T, Rotenberg E, Cohen-Hilaleh E, Raz-Yaseef N, Tatarinov F, Preisler Y, Ogée J, Cohen S, Yakir D. 2012. Quantifying transpirable soil water and its relations to tree water use dynamics in a water-limited pine forest. *Ecohydrology* **7**: 409–419.

Klein T, Rotenberg E, Tatarinov F, Yakir D. 2016. Association between sap flow-derived and eddy covariance-derived measurements of forest canopy CO_2 uptake. *New Phytologist* **209**: 436–446.

Klein T, Yakir D, Buchmann N, Grünzweig JM. 2014. Towards an advanced assessment of the hydrological vulnerability of forests to climate change-induced drought. *New Phytologist* **201**: 712–716.

Law BE, Falge E, Gu L, Bakwin P, Berbigier P, Davis K, Dolman AJ, Falk M, Fuentes JD, Goldstein A *et al.* 2002. Environmental controls over carbon

dioxide and water vapor exchange of terrestrial vegetation. *Agricultural and Forest Meteorology* **113**: 97–120.

Law BE, Williams M, Anthoni PM, Baldocchi DD, Unswort MH. 2000. Measuring and modelling seasonal variation of carbon dioxide and water vapour exchange of a *Pinus ponderosa* forest subject to soil water deficit. *Global Change Biology* **6**: 613–630.

Leuzinger S, Zotz G, Asshoff R, Körner C. 2005. Responses of deciduous forest trees to severe drought in Central Europe. *Tree Physiology* **25**: 641–650.

Maseda PH, Fernandez RJ. 2006. Stay wet or else: three ways in which plants can adjust hydraulically to their environment. *Journal of Experimental Botany* **57**: 3963–3977.

Maseyk KS. 2006. Ecophysiological and phonological aspects of *Pinus halepensis* in an arid-Mediterranean environment. PhD thesis, Weizmann Institute of Science, Rehovot, Israel.

Maseyk KS, Grünzweig JM, Rotenberg E, Yakir D. 2008b. Respiration acclimation contributes to high carbon-use efficiency in a seasonally dry pine forest. *Global Change Biology* **14**: 1553–1567.

Maseyk KS, Lin T, Rotenberg E, Grünzweig JM, Schwartz A, Yakir D. 2008a. Physiology–phenology interactions in a productive semi-arid pine forest. *New Phytologist* **178**: 603–616.

Maslov AD. 2010. *Koroyed-tipograf I usychanie yelovych lesov. "Bark printing beetle and drying up of spruce forest"*. Moscow, Russia: VNIILM (in Russian).

Moriana A, Villalobos FJ, Fereres E. 2002. Stomatal and photosynthetic responses of olive (*Olea europaea* L.) leaves to water deficits. *Plant, Cell & Environment* **25**: 395–405.

Neeman G, Trabaud L, eds. 2000. *Ecology, biogeography and management of* Pinus halepensis *and* P. brutia *forest ecosystems in the Mediterranean Basin.* Leiden, the Netherlands: Backhuys Pub.

Oren R, Sperry JS, Katul GG, Pataki DE, Ewers BE, Phillips N, Schäfer KVR. 1999. Survey and synthesis of intra- and interspecific variation in stomatal sensitivity to vapour pressure deficit. *Plant, Cell & Environment* **22**: 1515–1526.

Raz Yaseef N, Yakir D, Rotenberg E, Schiller G, Cohen S. 2010. Ecohydrology of a semi-arid forest: partitioning among water balance components and its implications for predicted precipitation changes. *Ecohydrology* **3**: 143–154.

Reichstein M, Bahn M, Ciais P, Frank D, Mahecha MD, Seneviratne SI, Zscheischler J, Beer C, Buchmann N, Frank DC *et al.* 2013. Climate extremes and the carbon cycle. *Nature* **500**: 287–295.

Reichstein M, Falge E, Baldocci D, Papale D, Aubinet M, Berbigier P, Bernhofer Ch, Buchmann N, Gilmanov T, Granier A *et al.* 2005. On the separation of net ecosystem exchange into assimilation and ecosystem respiration: review and improved algorithm. *Global Change Biology* **11–3**: 1424–1439.

Reichstein M, Tenhunen JD, Roupsard O, Ourcival J-M, Rambal S, Miglietta F, Peressotti A, Pecchiari M, Tirone G, Valentini R. 2002. Severe drought effects on ecosystem CO_2 and H_2O fluxes at three Mediterranean evergreen sites: revision of current hypotheses? *Global Change Biology* **8**: 999–1017.

Reyer CPO, Leuzinger S, Rammig A, Wolf A, Bartholomeus RP, Bonfante A, de Lorenzi F, Dury M, Gloning P, Abou Jaoudé R *et al.* 2013. A plant's perspective of extremes: terrestrial plant responses to changing climatic variability. *Global Change Biology* **19–1**: 1365–2486.

Rotenberg E, Yakir D. 2010. Contribution of semi-arid forests to the climate system. *Science* **327**: 451–454.

Ruehr NK, Law BE, Quandt D, Williams M. 2014. Effects of heat and drought on carbon and water dynamics in a regenerating semi-arid pine forest: a combined experimental and modeling approach. *Biogeosciences* **11**: 4139–4156.

Saatchi S, Asefi-Najafabady S, Malhi Y, Aragão LEOC, Anderson LO, Myneni RB, Nemani R. 2013. Persistent effects of a severe drought on Amazonian forest canopy. *Proceedings of the National Academy of Sciences, USA* **110**: 565–570.

Schiller G. 2011. The case of Yatir Forest. In: Bredemeier M, Cohen S, Godbold DL, Lode E, Pichler V, Schleppi P, eds. *Forest management and the water cycle: an ecosystem-based approach. Ecological Studies* **212**: 163–186.

Shvidenko AZ, Schepaschenko DG. 2013. Climate change and wildfires in Russia. *Contemporary Problems of Ecology* **6**: 683–692.

Tuzov VK. 2013. *"Outbreak of bark beetle in European part of Russia and measures for eliminate its consequences". Problems of dying of spruce stands.* Proceedings of International Scientific and Practical Seminar, 26–27 September 2013, Mogilyov, Belarus. Minsk, Belarus: Colorpoint Publishers, 22–24.

Ungar ED, Rotenberg E, Raz-Yaseef N, Cohen S, Yakir D, Schiller G. 2013. Transpiration and annual water balance of Aleppo pine in a semiarid region: implications for forest management. *Forest Ecology and Management* **298**: 39–51.

Weinstein A. 1989. Geographic variation and phenology of *Pinus halepensis, P. brutia* and *P. eldarica* in Israel. *Forest Ecology and Management* **27**: 99–108.

Winstanley D. 1972. Sharav. *Weather* **27**: 146–160.

Supporting Information

Additional supporting information may be found in the online version of this article.

Table S1 Comparison of different hamsin detection algorithms with manual detection for the years 2001–2007

Methods S1 Detection of hamsin events.

Notes S1 Results of comparison of hamsin detection by different methods.

Please note: Wiley Blackwell are not responsible for the content or functionality of any supporting information supplied by the authors. Any queries (other than missing material) should be directed to the *New Phytologist* Central Office.